PEPTIDES 29 (2008) 1633–1644

available at www.sciencedirect.com

ScienceDirect

journal homepage: www.elsevier.com/locate/peptides

Solution NMR structures of the antimicrobial peptides phylloseptin-1, -2, and -3 and biological activity: The role of charges and hydrogen bonding interactions in stabilizing helix conformations

Jarbas M. Resende [a,b], *Cléria Mendonça Moraes* [a,b], *Maura V. Prates* [c], *Amary Cesar* [a], *Fabio C.L. Almeida* [d], *Nathália C.C.R. Mundim* [c,e], *Ana Paula Valente* [d], *Marcelo P. Bemquerer* [c], *Dorila Piló-Veloso* [a], *Burkhard Bechinger* [b,*]

[a] *Universidade Federal de Minas Gerais, Departamento de Química, Avenida Presidente Antonio Carlos 6627, 31270-901 Belo Horizonte, MG, Brazil*

[b] *Université Louis Pasteur/CNRS, UMR7177, Institut de Chimie, 4, rue Blaise Pascal, 67000 Strasbourg, France*

[c] *EMBRAPA, Recursos Genéticos e Biotecnologia, PqEB, Av.W5 Norte (final), 70770-900 Brasília, DF, Brazil*

[d] *Universidade Federal do Rio de Janeiro, CNRMN, Departamento de Bioquímica Médica, Av. Brigadeiro Trompowiski s/n, CCS, 21941-590 Rio de Janeiro, RJ, Brazil*

[e] *Universidade de Brasília, Instituto de Biologia, Campus Universitário Darcy Ribeiro – Asa Norte, cep 70910-900 Brasília, DF, Brazil*

ARTICLE INFO

Article history:
Received 30 April 2008
Received in revised form
12 June 2008
Accepted 16 June 2008
Published on line 4 July 2008

Keywords:
Amphipathic α-helix
Antibiotic
Antifungal
Helix capping
Hydrogen bonds
Membrane interactions
Helix dipole

ABSTRACT

Phylloseptins are antimicrobial peptides of 19–20 residues which are found in the skin secretions of the *Phyllomedusa* frogs that inhabit the tropical forests of South and Central Americas. The peptide sequences of PS-1, -2, and -3 carry an amidated C-terminus and they exhibit 74% sequence homology with major variations of only four residues close to the C-terminus. Here we investigated and compared the structures of the three phylloseptins in detail by CD- and two-dimensional NMR spectroscopies in the presence of phospholipid vesicles or in membrane-mimetic environments. Both CD and NMR spectroscopies reveal a high degree of helicity in the order PS-2 ≥ PS-1 > PS-3, where the differences accumulate at the C-terminus. The conformational variations can be explained by taking into consideration electrostatic interactions of the negative ends of the helix dipoles with potentially cationic residues at positions 17 and 18. Whereas two are present in the sequence of PS-1 and -2 only one is present in PS-3. In conclusion, the antimicrobial phylloseptin peptides adopt alpha-helical conformations in membrane environments which are stabilized by electrostatic interactions of the helix dipole as well as other contributions such hydrophobic and capping interactions.

* *Corresponding author at*: Faculté de chimie, Institut le Bel, 4, rue Blaise Pascal, 67070 Strasbourg, France. Tel.: +33 3 90 24 51 50; fax: +33 3 90 24 51 51.
E-mail address: bechinger@chimie.u-strasbg.fr (B. Bechinger).

Abbreviations: CFU, colony forming units; DQF-COSY, double-quantum filtered correlation spectroscopy; HSQC, heteronuclear single-quantum coherence; NMR, nuclear magnetic resonance; NOESY, nuclear Overhauser effect spectroscopy; PS-1, phylloseptin-1; PS-2, phylloseptin-2; PS-3, phylloseptin-3; POPC, 1-palmitoyl-2-oleoyl-*sn*-glycero-3-phosphocholine; POPS, 1-palmitoyl-2-oleoyl-*sn*-glycero-3-phospho-L-serine; TFE, 2,2,2-trifluoroethanol; TOCSY, total correlation spectroscopy; wt, wild type.

0196-9781/$ – see front matter © 2008 Elsevier Inc. All rights reserved.
doi:10.1016/j.peptides.2008.06.022

1. Introduction

The increasing resistance of pathogens against many commonly used antibiotics requires the continuous research and development of new bactericidal and fungicidal compounds [50,28]. Both plants and animals produce, store and secrete antibiotic peptides in exposed tissues, or synthesize such compounds upon induction, thereby a defense system is established that can be set into action immediately when infections occur [76,12]. Therefore, one approach consists in the search and investigation of naturally occurring antibiotic compounds, understanding their mechanism of action and using them as templates for the design of new therapeutics [7]. Indeed, although antibiotic peptides have been isolated from amphibians or insects already in the 1960s interest in this field of research has been increasing over the past decades [41,56]. Today almost 1000 antimicrobial sequences are compiled in the corresponding databases (http://www.bbcm.univ.trieste.it/~tossi/amsdb.html; http://aps.unmc.edu/AP/main.php).

Some of the best studied linear peptide antibiotics are those that are found in amphibian skins and research is continuously ongoing to find and characterize new compounds from frogs and other species [3,13]. Many of these molecules are cationic and exhibit amphipathic properties when interacting with membranes. Nevertheless, frog skin antimicrobial peptides can present relevant variation in sequence and three-dimensional structure and can thus be grouped into different families [62].

Membrane interactions are known to play an important role during antibiotic action of cationic antimicrobial peptides either by disruption and pore formation [7,9], or by allowing the peptides' passage into the cell interior where they can interact with other macromolecular targets [29,14]. The detailed mechanisms of how these peptides permeabilize and pass biological membranes remain a matter of debate [7,60,9], however, there is good agreement that the peptides are attracted by the bacterial membranes by electrostatic interactions and undergo conformational changes during membrane interactions. It is therefore necessary to study the conformations of these peptides as well in aqueous buffers as in membrane-mimetic environment to be able to follow the conformational changes and to understand their biological activities. As some of the peptides seem to also interact with internal targets [55] additional biophysical and structural investigations might become necessary to characterize such complexes.

Phylloseptins are antimicrobial peptides found in the skin secretions of hylids from the *Phyllomedusa* genus (anura) that inhabit tropical forests of South and Central Americas. They consist of 19 or 20 highly conserved residues and carry an amidated C-terminus [41], a modification which has been shown to promote biological activity of other sequences [2,36]. The phylloseptin-1, -2, and -3 peptides (PS-1, PS-2, and PS-3 – Table 1) were isolated from *Phyllomedusa hypochondriallis*, a frog species found in Brazilian Southeast Atlantic forests [41].

Most linear cationic peptides, including phylloseptins, exhibit broadband antimicrobial activities [64,75]. Nevertheless, the detailed spectrum of antibiotic and antifungal activities varies with their amino acid sequence, and it seems that the detailed peptide composition and structure reflect adaptations of the species to their microenvironment. Considerable differences in biological activities have been observed upon relatively small modifications of primary sequence of model compounds, even when the overall amino acid composition of the peptide has been kept constant [71,45].

Table 1 – The primary sequences of the phylloseptins investigated in this paper: the residues with the potential to carry a positive charge at neutral pH are shown in bold

PS-1	FLSLI P**H**AIN AVSAI A**KH**N-NH_2
PS-2	FLSLI P**H**AIN AVSTL V**HH**F-NH_2
PS-3	FLSLI P**H**AIN AVSAL AN**H**G-NH_2

In this regard the phylloseptins provide an interesting example as a number of variants exist with small differences in amino acid composition. The three peptides studied here are characterized by 74% sequence homology and they all carry two histidine residues at positions 7 and 18 (Table 1). However, they differ in the amino acid compositions of residues 14–17 and 19. The most pronounced difference is the variation of the effective charge of residue 17 at physiological pH. Whereas PS-1 carries a lysine (+1), a histidine is located at the same position of PS-2 (0 to +1), and an asparagine at PS 3 (charge neutrality).

This peptide system is therefore of interest to follow the structural modifications due to these differences and to compare them to the antibiotic activities against well-characterized pathogenic microorganisms. Understanding the structure–function relationship of antimicrobial peptides in sufficient detail will help in the rational design of cheaper and more efficient analogues [33,44]. In particular, the phylloseptins provide a test case how electrostatic interactions can modulate the structural features of linear peptides in membrane-mimetic environments.

In this paper we present studies comparing the antimicrobial activities of phylloseptin-1, -2, and -3 against several microorganisms, including bacteria and fungi. By using circular dichroism and two-dimensional solution NMR spectroscopy in aqueous buffer and in membrane-mimetic solvents [74,19] their biological activities could be compared with their detailed three-dimensional structures.

2. Materials and methods

2.1. Materials

TFE was from Aldrich Inc., TFE-d_2 was from Cambridge Isotopes Laboratories. POPC and POPS were from Avanti Polar Lipids (Birmingham, AL). Amino acid derivatives and other reagents for peptide synthesis were from NovaBiochem-Merck (Darmstadt, Germany).

2.2. Peptide synthesis

The peptides, with amidated C-terminus, were synthesized by solid-phase peptide synthesis on a Rink amide resin (0.61 mmol g^{-1}) by using the Fmoc/*t*-butyl strategy [20]. Couplings were performed with *N*,*N*′-diisopropylcarbodiimide/1-hydroxybenzotriazole in *N*,*N*-dimethylformamide for

60–120 min. Cleavage and final deprotection were conducted with trifluoroacetic acid (TFA):triisopropylsilane:ethanedithiol (90:5:5, v:v:v) for 90 min at room temperature. The peptide products were precipitated with diisopropyl ether, extracted with water and lyophilized.

2.3. Peptide purification

Synthetic peptides were purified by RP-HPLC (Shimadzu LC10 VP Series, Kyoto, Japan) using a preparative C_{18} column (Vydac 218TP1022, 22 × 250 mm, Hesperia CA, USA). A gradient from 5% to 95% of acetonitrile containing TFA 0.1% (solvent B) was applied, where solvent A was ultra-pure H_2O containing TFA 0.1%. The purified peptides were sequenced by MALDI-TOF–TOF mass spectrometry (Bruker Daltonics Inc. Ultraflex II, Bremen, Germany). Samples were co-crystallized from a saturated solution in the presence of an α-cyano-4-hydroxycinnamic acid matrix and in a 25% aqueous acetoniltrile solution containing 3% TFA. The MS and MS/MS spectra were obtained using the reflector mode with external calibration (data not shown).

2.4. Antimicrobial activity

Four human pathogenic bacterial strains, *Pseudomonas aeruginosa* ATCC 29853, *Klebsiella peneumoniae* ATCC 13853, *Staphylococcus aureus* ATCC 29213, *Escherichia coli* ATCC 24922, four bacterial and one yeast strains isolated from cows and humans contaminated with mastitis, *P. aeroginosa* wild type (wt), *Acinetobacter calcoaceticus* wt, *S. ureus* wt, *Streptococcus agalactiae* wt, and *Candida albicans* wt, were used to investigate the phylloseptin-1, -2, and -3 antimicrobial activities. Microorganisms were grown in stationary culture at 37 °C and transferred to the Mueller–Hinton liquid medium (National Committee for Clinical Laboratory Standards (NCCLS)-approved standard M100-S9) in which the tests were performed [67]. The bacterial liquid growth inhibition assay was performed as described by Bulet et al. [15]. The peptides were dissolved and diluted 8-fold in Mueller–Hinton broth. The highest peptide concentration used for the assay was 128 μg/mL. The initial inoculum was 2.5×10^8 colony forming units (CFU)/mL (0.5 in the McFarland scale) and 2.5×10^5 CFU/mL. The final volume was 100 μL, 50 μL of the peptide solution in broth, 50 μL of the inoculum in Mueller–Hinton broth. The experiment was carried out in stationary culture at 37 °C, and the spectrophotometer readings were performed 12 h after incubation. The minimal inhibitory concentration, as introduced by Park et al. [51], was measured from optical density (A_{595}) and was the result of three independent measurements. Conventional antibiotics (amoxicillin, ceftazidime, trimethoprim, tetracycline, cephazoline, penicillin G or benzyl-penicillin and levofloxacin) and antifungals (amphotericin B, fluconazole, itraconazole, myconazole and ketoconazole) had their minimal inhibitory concentrations determined against the six experimental bacterial strains by automated biochemical analysis (Vitek, bioMerieux Inc.).

2.5. CD measurements

CD spectra were recorded at 20 °C using a Jasco spectropolarimeter J-810 coupled to a Peltier Jasco PFD-425S system for temperature control. The spectra were analyzed using the CDPro software [63].

Solutions of the peptides at 0.1 mg/mL in different TFE:buffer mixtures (0:100, 10:90, 30:70, and 60:40 v/v) were prepared with 10 mM phosphate buffer, pH 7.0. Alternatively, samples of peptides and small unilamellar POPC:POPS 3:1 (mole/mole) vesicles were prepared at peptide:lipid ratio of 1:55 and a final peptide concentration of 0.09 mg/mL. To ensure homogenous mixing the appropriate amounts of lipid and peptide were dissolved in organic solvents (peptide and POPC in TFE and POPS in dichloromethane), the two solutions were mixed, the bulk of the solvent removed under a stream of nitrogen gas and the remaining traces of solvent by exposure to high vacuum for 15 h. Large multilamellar vesicles (MLV) were formed from the dry lipid–peptide film by the addition of buffer (5 mM NaH_2PO_4/Na_2HPO_4, pH 7.0) and vortexing. The samples were equilibrated by three cycles of vortexing, freezing, thawing and tip sonication for about 30 min (Bandelin, Sonorex super RK 514 BH; Berlin, Germany). Small unilamellar vesicles (SUV) were prepared by extrusion through polycarbonate filters of 50 nm pore size (Avestin Inc., Ottawa, Canada).

Spectra were collected from 190–260 nm or 195–260 nm in TFE/water and in the presence of vesicles, respectively, using a quartz cell with a path length of 1 mm. The following parameters were employed: scan speed 50 nm/min, data pitch 0.2 nm, 1 s response, 1 nm band width, and 8 scans. Similar experiments with the respective blank solutions were also carried out in order to allow for background subtraction.

2.6. Two-dimensional solution NMR spectroscopy

Two-dimensional solution NMR experiments were carried out in order to determine the three-dimensional structure of the antibiotic peptides. The samples were prepared by dissolving the peptides in a mixture of TFE-d_2/H_2O (60:40, v/v) at 4.0 mM concentrations. The pH was adjusted to 7.0 with 20 mM aqueous phosphate buffer. The total correlation spectroscopy (TOCSY), nuclear Overhauser effect spectroscopy (NOESY) and heteronuclear single-quantum coherence (HSQC) solution NMR experiments were performed at 20 °C on a Bruker Avance DRX spectrometer operating at a ^1H frequency 600.043 MHz. A 5 mm triple-resonance ($^1H/^{13}C/^{15}N$) gradient probe was used. Water suppression was achieved using the pre-saturation technique. All NMR spectra were processed using NMRPIPE [24].

Total correlation spectroscopy spectra were acquired using the MLEV-17 pulse sequence [6]. The spectral width was chosen to be 6900 Hz, 512 t_1 increments were collected with 8 transients of 4096 points for each free induction decay. NOESY spectra [39] were acquired using mixing times of 100, 150, 200, 300 and 400 ms to check for spin diffusion. The spectral width was set to 6900 Hz, 512 t_1 increments were collected with 16 transients of 4096 points for each free induction decay. $^1H–^{13}C$ HSQC spectra were acquired with F1 and F2 spectral widths of 27160 and 8993 Hz, respectively. 400 t_1 increments were collected with 56 transients of 1024 points for each free induction decay. The experiment was acquired in an edited mode [72]. $^1H–^{15}N$ HSQC spectra were acquired with F1 and F2 spectral widths of 27160 and 8993 Hz, respectively. Eighty t_1 increments were collected with 400 transients of 1024 points

Table 2 – Minimal inhibitory concentrations determined for PS-1, PS-2, and PS-3 in the presence of ATCC bacteria in 10^5 and 10^8 CFU inoculums

Bacteria (ATCC strains)	MIC (μM)[a]					
	PS-1	PS-2	PS-3	Amoxicillin	Ceftazidime	Trimethoprim
S. aureus[c]	31.7	15.1	32.9	NDA[b]	NDA	>441.4
E. coli[c]	63.4	60.4	65.6	691.9	465.5	441.4
K. pneumoniae[c]	31.7	60.4	65.6	345.9	232.7	220.7
P. aeruginosa[c]	63.4	60.4	65.6	NDA	NDA	110.3
S. aureus[d]	3.9	1.9	4.1	NDA	NDA	<110.3
E. coli[d]	1.9	3.7	4.1	88.9	59.3	<27.6
K. pneumoniae[d]	1.9	3.7	4.1	44.4	<29.1	27.6
P. aeruginosa[d]	7.9	7.6	8.2	NDA	NDA	<3.4

CFU, colony forming units.
[a] MIC, minimal concentrations of peptide required for the total inhibition of cell growth in liquid medium. These analyses were performed according to the recommendations of NCCLS. Experiments were performed in triplicates.
[b] NDA, no detectable activity.
[c] Initial inoculum of 10^8 cells/mL.
[d] Initial inoculum of 10^5 cells/mL.

for each free induction decay [72]. DQF-COSY spectra [52,25] have been acquired on a Bruker Avance DRX-400 spectrometer. A spectral width of 4005 Hz was employed and 1024 t_1 increments of 4096 data points have been collected for each free induction decay. Water suppression was achieved by double-quantum filtering [52], the Watergate sequence [53] and by employing pre-saturation during the relaxation delay.

2.7. NOE data and structure calculations

The NMR spectra were analyzed using NMRVIEW, version 5.0.3 [35]. NOE intensities obtained at 200 ms mixing times were converted into semi-quantitative distance restrains using the calibration by Hyberts et al. [34]. The upper limits of the distances restrains thus obtained were 2.8, 3.4, and 5.0 Å (strong, medium, and weak NOE, respectively). Structure calculations were performed using the Xplor-NIH software, version 2.17.0 [58]. Starting with an extended conformation, 200 structures were generated using a simulated annealing protocol. This was followed by 18000 steps of simulated annealing at 1000 K and a subsequent decrease in temperature in 9000 steps in the first slow-cool annealing stage. The stereochemical quality of the lowest energy structures was analyzed by PROCHECK-NMR [40]. The display, analysis, and manipulation of the three-dimensional structures were performed with the program MOLMOL [37]. The atomic coordinates of the most stable structures have been deposited in the RCSB Protein Data Bank, http://www.rcsb.org/pdb/home/home.do (PDB ID codes: 2JQ0 for PS-1, 2JPY for PS-2, and 2JQ1 for PS-3).

3. Results

3.1. Antimicrobial activity

Whereas, it has been demonstrated previously that at micromolar concentrations phylloseptin PS-1 is a broad-spectrum antimicrobial peptide that inhibits the growth of Gram-negative and Gram-positive bacteria as well as of filamentous yeast [41], here we investigated the antimicrobial activities of the three phylloseptin peptides against a much wider variety

Table 3 – Minimal inhibitory concentrations determined for PS-1, PS-2, and PS-3 in the presence of wt bacteria and yeast in 10^8 CFU inoculum

Bacteria	MIC (μM)[a]						
	PS-1	PS-2	PS-3	Tetracycline	Cephazolin	Benzylpenicillin	Levofloxacin
P. aeruginosa wt	31.7	60.4	32.8	NDA[b]	71.1	96.9	NDA
A. calcoaceticus wt	7.9	3.7	4.1	NDA	71.1	96.9	22.2
S. aureus wt	15.8	7.6	8.2	36.4	17.8	48.5	2.8
S. agalactiae wt	3.9	1.9	4.1	36.4	17.8	3.0	2.8
Yeast				Amphotericin B	Fluconazole	Itraconazole	Myconazole	Ketoconazole
C. albicans wt	7.9	15.1	8.2	4.4	25.8	5.6	9.5	30.2

CFU, colony forming units; wt, wild type microorganisms; initial inoculum of 10^8 cells/mL.
[a] MIC, minimal concentrations of the peptides required for the total inhibition of cell growth in liquid medium. These analyses were performed according to the recommendations of NCCLS. Experiments were performed in triplicates.
[b] NDA, no detectable activity.

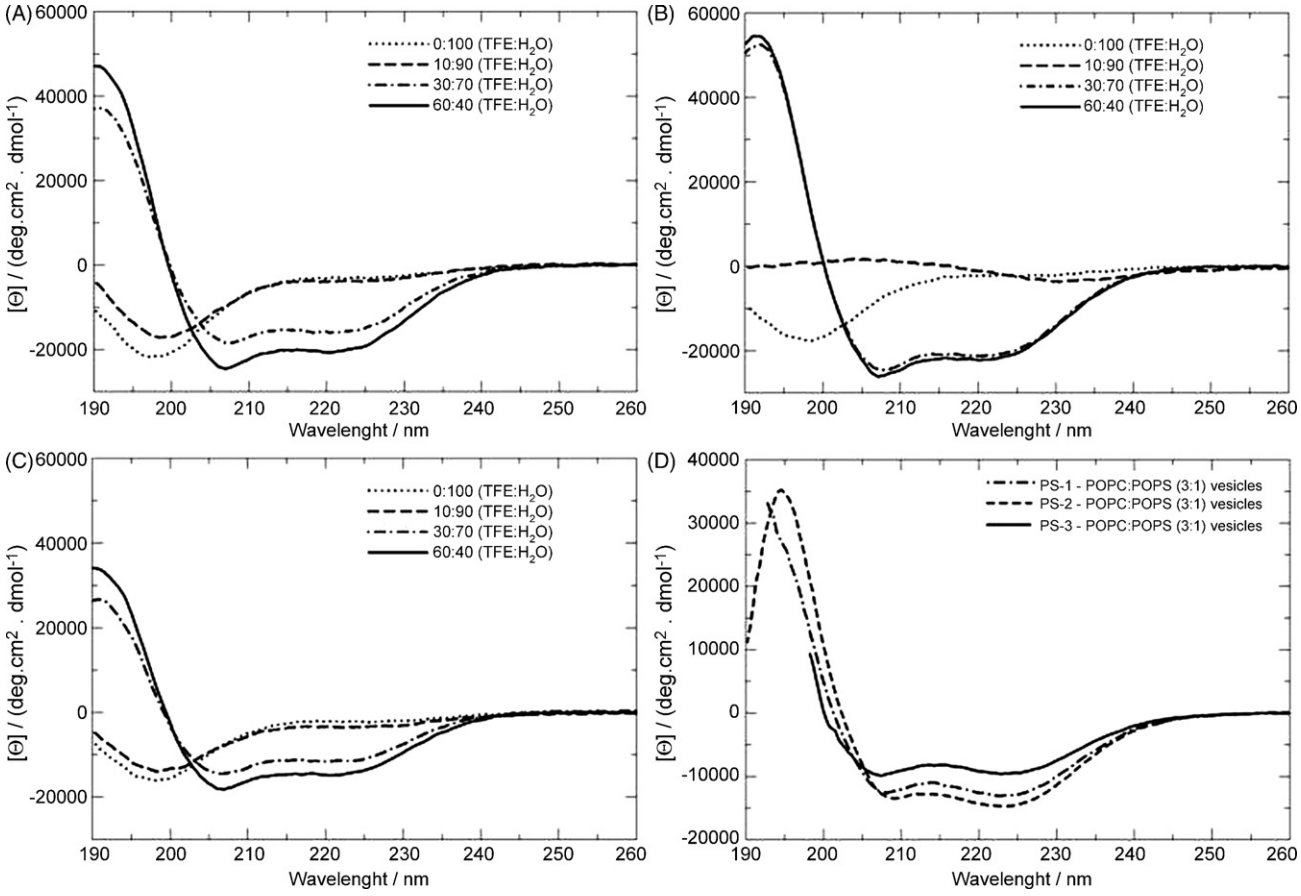

Fig. 1 – CD spectra of PS-1 (A), PS-2 (B), and PS-3 (C) in 10 mM phosphate buffer, pH 7.0 (dotted line), 10%TFE (dashed line), 30%TFE (dashed-dotted line), and 60%TFE (solid line). (D) CD spectra of PS-1 (dashed-dotted line), PS-2 (dashed line), and PS-3 (solid line) in the presence of small unilamellar vesicles of POPC: POPS (3:1 mole/mole). At short wave length (<200 nm) light scattering artifacts strongly increase in the presence of lipid vesicles. In these cases only the spectral component used for the analysis are shown.

of microorganisms including pathogenic bacteria. The synthetic PS sequences studied were tested using bacterial inocula of 10^5 and 10^8 CFU and all exhibit potent antimicrobial activities (Tables 2 and 3). At the same time these peptides display insignificant activity against human red blood cells, where PS-1 and PS-2 exhibit only about 2% total lysis at the concentrations required for antibiotic activity [41].

3.2. *CD spectroscopy*

Cationic antimicrobial peptides have been shown to interact with biological membranes where they show pore-forming and cell-penetrating activities (review e.g. [7]). Therefore, the structure and interactions of phyloloseptins 1, 2, and 3 were investigated in membrane-mimetic environments using CD spectroscopy. The CD spectra of the three peptides in aqueous buffer and in TFE/water mixtures are shown in Fig. 1A–C. Whereas the spectra of phylloseptins in aqueous buffer are characteristic of random coil conformations, their degree of α-helix secondary structures strongly increases when the amount of TFE is augmented in a step-wise manner.

At TFE ratios ≥30%, two minima close to 208 and 222 nm are clearly visible for all peptides, characteristic of helical conformations [22]. Whereas for PS-1 and PS-3 these intensities become even more pronounced when the TFE content is further increased to 60%, the degree of helicity remains constant between 30% and 60% TFE for PS-2. The quantitative analysis and deconvolution of the curves using the CDPro software indicate helical contents of 53%, 75%, and 41% (30% TFE) and 70%, 78%, and 53% (60% TFE) for PS-1, PS-2, and PS-3, respectively.

In the presence of POPC:POPS (3:1 mole/mole) vesicles the CD spectra of phylloseptins are also indicative of a high content of helix conformations, albeit the contributions of this secondary structure is reduced when compared with the spectra obtained at 60% TFE (Fig. 1D). This is probably due to the fast exchange of peptides between the membrane-associated (helical) and water-soluble states (random coil) in the bilayer systems and similar observations have been made in previous investigations of cationic antimicrobial peptides (compare e.g. [42] with [26]).

3.3. *Two-dimensional solution NMR spectroscopy*

Sequence-specific chemical shift assignments have been performed for phylloseptins from the correlations observed

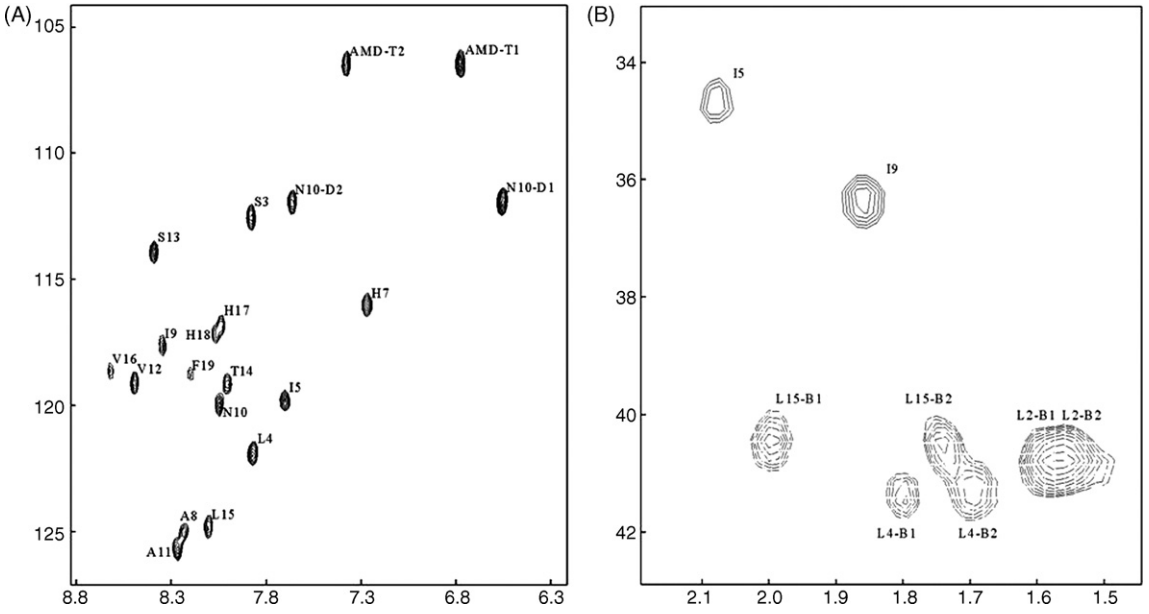

Fig. 2 – Selected spectral regions are shown of the (A) $^{1}H–^{15}N$ HSQC and (B) $^{1}H–^{13}C$ HSQC spectra of PS-2 at 4.0 mM in TFE:H_2O (40:60 v/v) – pH 7.0 (phosphate buffer) at 20.0 °C. In (B) the solid lines represent peaks with positive phase whereas dotted lines indicate negative intensities.

in TOCSY and NOESY spectra using standard procedures [74]. The $^{1}H–^{15}N$ and $^{1}H–^{13}C$ HSQC spectra provided a control and allowed to unequivocally assign CH β protons of isoleucine and the CH_2 β protons of leucine residues, as illustrated in Fig. 2. The high number of cross-peaks detected in the NOESY spectra (Fig. 3) indicates well-folded peptide conformations. In particular correlations of the sort NN(i,i + 1), αN(i,i + 3), αβ (i,i + 3) and αN (i,i + 4) (Fig. 4A–C) suggest the existence of helical conformations. By analyzing Fig. 4B, one observes that PS-2 presents α-helical conformations ranging from the fifth residue to the C-terminal amide. Additional dαN(i,i + 1) contacts indicate some less regular structure also for residues 3–5. On the other end NOE correlations involving the terminal amide proton suggest that the C-terminal amidation plays an important role in the high degree of order observed for this peptide.

Fig. 4A indicates that PS-1 is also characterized by a high degree of α-helical structure, whereas the number of inter-residue NOEs of PS-3 is indicative that this latter peptide is less structured in particular at its most C-terminal region (Fig. 4C). Fig. 4D–F present the difference between the experimental α-carbon chemical shifts and the standard values for a random coil peptide [73]. The positive values between the 5th and the 18th amino acid residues confirm that PS-1 and PS-2 adopt helical conformations involving these residues and a shorter helical domain for PS-3 (residues 5–15). Furthermore, the NOE connectivities and Cα chemical shifts suggesting helical conformations in the central portions of the peptides correlate well with $^{3}J_{HN–HA}$ couplings <6 Hz which predominate in these regions (Fig. 4A–C [74]).

The ten lowest energy structures obtained after simulated annealing are shown in Fig. 5 and the differences between the peptides already observed when the NOEs and chemical shifts have been analyzed (Fig. 4) become obvious in these atomic models. Notably, all three peptides exhibit strongly amphipathic structures. This effect is most pronounced for PS-2 where all polar residues of the helix are found on one face of the helix whereas the other face is composed exclusively of apolar residues. When compared with PS-2, PS-1 is less amphipathic due to the exchange of Thr-14 by an alanine within the polar side of the peptide. In a similar manner the C-terminal asparagine in PS-1 substitutes for a phenylalanine of PS-2 and resides within the apolar face of the helix. Interestingly, PS-2 shows additional NOEs characteristics of helical structure involving the protons of the C-terminal amide indicating that the 19th amino acid residue of PS-2 is part of the helical segment. These NOEs are absent for PS-1 (Fig. 4).

The statistics of the structural analysis of phylloseptin-1, -2, and -3 are summarized in Table 4. The RMSD values obtained for all residues are suggestive of considerable conformational flexibility, however, these values significantly drop when only the helical fragments are taken into account. Most of the ϕ and ψ angles are found in the most favored or in the additionally allowed regions of the Ramachandran plot indicating the good quality of the structures.

4. Discussion

The CD- and multidimensional NMR investigation indicate that phylloseptin-1, -2, and -3 exhibit random coil conformations in aqueous solution and adopt continuous helix conformations in membrane environments. Similar structural transitions have been observed with other cationic linear peptides [42,31,10,33] and the findings with phylloseptins are therefore in line with previous models that describe the membrane interactions and biological activities of cationic

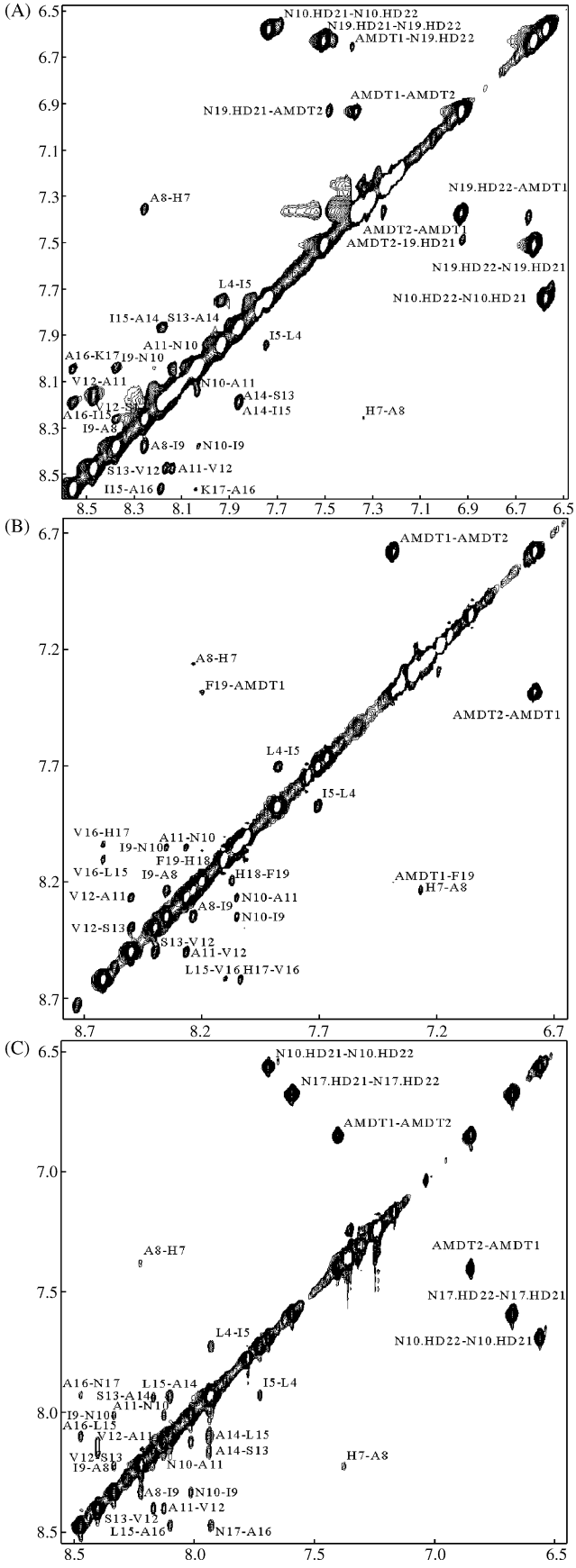

Fig. 3 – Amide–amide regions of the NOESY spectra of (A) PS-1, (B) PS-2, and (C) PS-3 at 4.0 mM in TFE:H_2O (40:60) – pH 7.0 (phosphate buffer), 20.0 °C.

antimicrobial peptides [46,7,59,32,76]. The helical structures exhibit a highly amphipathic character which allows these peptides to efficiently partition into the membrane interface. In this manner they can develop membrane-destabilizing and pore-forming activities (reviewed in [59,76,9]). The peptides exchange between the aqueous solution and the membrane, and electrostatic interactions help to increase membrane association with acidic phospholipid bilayers [38,47,8].

Notably, despite the sequence similarity considerable differences in the degree of helix formation are observed close to C-terminus when the structures of phylloseptin-1, -2, and -3 are compared with each other (Fig. 5). The solution NMR data and the resulting structures indicate that the helical segments involve residues 5–18 for PS-1, 5–19 for PS-2, and 5–15 for PS-3, which corresponds to a degree of helicity of 74% for PS-1, 79% for PS-2, and 58% for PS-3. The qualitative CD structural analysis is in excellent agreement with the NMR data with very similar results when the helix content in 60% TFE was analyzed. Helix formation in the presence of small unilamellar vesicles follows the same trend, i.e. PS-2 $\geq$ PS-1 $>$ PS-3. Therefore, in TFE/water mixtures the structures of the membrane-associated peptides are well represented and, even more importantly, the differences between the different helix-forming propensities of the three-phylloseptin peptides are maintained in this environment.

Major differences between the PS-3 structure and those of PS-1 and PS-2 are consistently observed in the C-terminal portion of these peptides, which correlates with the differences between the peptides' primary sequences starting from the 14th amino acid residue. When the amino acid composition of residues 14–19 is taken into consideration the overall hydrophobicity of PS-1 and PS-3 closely match each other whereas that of PS-2 is clearly different [69]. However, when the amino acids that potentially carry a positive charge at physiological pH are considered a better correlation with the structural data is obtained. Whereas PS-3 has only one basic residue in this region (His-18), two are found for PS-1 and PS-2 (Lys-17/His-18 for PS-1 and His-17/His-18 for PS-2). This observation suggests that electrostatic interactions between these cationic side chains and the negative end of the helix dipole stabilize and promote helical conformations at the C-terminus. This effect is least pronounced for PS-3 which carries a polar but uncharged asparagine at position 17. The H2 and H4 protons of the histidine 18 side chains of all three peptides and of histidine 17 of PS-2 exhibit chemical shift frequencies in the intermediate range (Fig. 6) suggesting a partially charged state of these side chains at pH 7 [43,57,1]. Our results suggest that although removal of the negative charge of the terminal carboxyl by amidation helps to stabilize the C-terminal helix other favorable interactions are required to extend the helix to the very last residue. In previous investigations the interactions of the helix dipole with a positively charged side chain, and histidine in particular, positioned at the C-terminus of the helix have been shown to have helix stabilizing properties [17,18,4].

The close distances between the aromatic side chains His-17–His-18 and His-18–Phe-19 in the calculated PS-2 structures suggest that other helix stabilizing interactions at the C-terminus derive from aromatic stacking involving these three residues [49]. The aromatic shielding of His-18 in

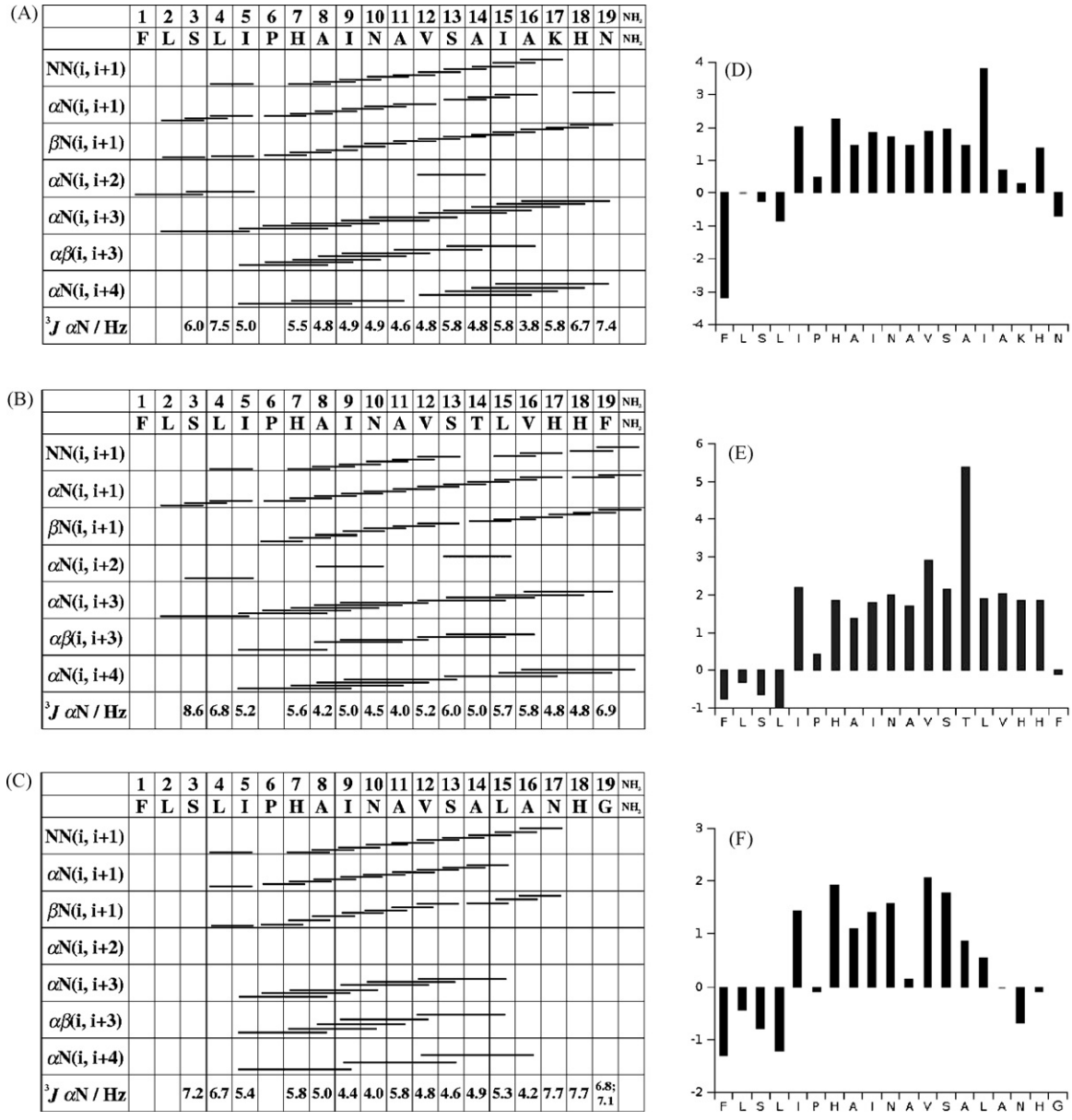

Fig. 4 – Graphical summary of NOEs and $^{3}J_{HN-HA}$-couplings characteristics of secondary structure observed for PS-1 (A), PS-2 (B), and PS-3 (C) and differences between the experimental α-^{13}C chemical shifts and the random coil values for (D) PS-1, (E) PS-2, and (F) PS-3.

PS-2 is also obvious when the H4 chemical shift is taken into consideration (Fig. 6). The unusual increase in the chemical shift of the alpha carbons of PS-2 Thr-14 and of PS-1 Ile-15 (Fig. 4D and E) probably also derive from the proximity of those aromatic side chains. Significant energy contributions to helix stabilization have previously been derived for cation–aromatic and aromatic–aromatic interactions [61,16,11], although the details how the aromatic side chains interact with each other remain a matter of discussion [49,65,21]. Although several NOEs restrain the His-18 and Phe-19 of PS-2 in a proximal arrangement, their number is insufficient to determine if these side chains adopt a stacked or T-shaped structure, or exhibit conformational exchange between such structures.

Due to the amino acid composition aromatic interactions are considerably less important in PS-1 than in the other two peptides and a different set of interactions must contribute to the stabilization of its C-terminal helix. Indeed when the sequence is analyzed in detail residues 14–19 are well positioned for helix capping as each of them exhibits a high 'normalized positional residue frequency' when histidine 18 is considered to be the helix terminus [5]. In this capping arrangement the helix can be stabilized by a hydrogen bonding interaction of the Asn-19 side chain amide protons with upstream carbonyls.

In addition, the structure calculations are indicative that the PS-2 helix is stabilized by H-bonding interactions between the C═O of residue 16 and the C-terminal amide group. In previous

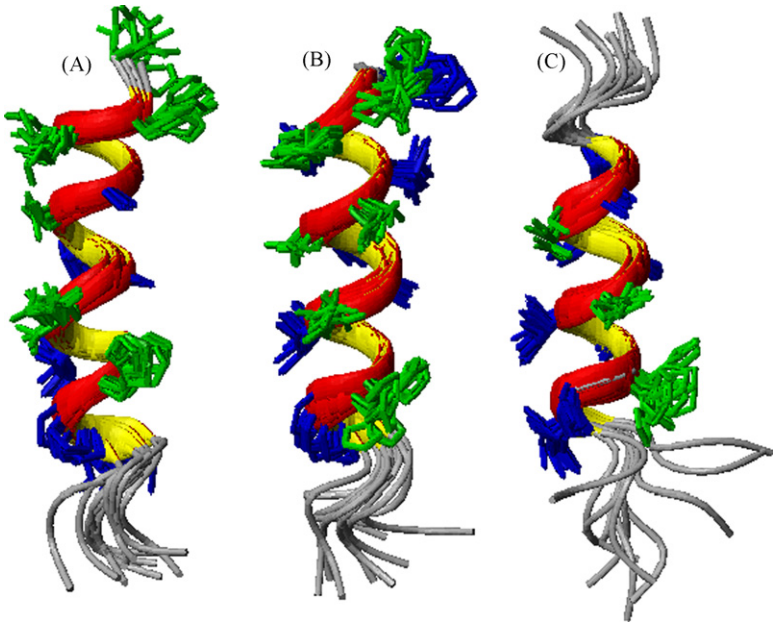

Fig. 5 – Ten lowest energy structures of (A) PS-1 (superposition of residues 5–19), (B) PS-2 (superposition of residues 5–19), and (C) PS3 (superposition of residues 5–15). Hydrophilic residues are shown in green and hydrophobic residues in blue. The N-termini are facing down.

papers H-bonding interactions have also been found important in stabilizing the helix C-terminus, including uncharged histidines [4], prolines [54] or other helix capping motifs [5].

In summary, electrostatic interactions between the positive charges of lysines and histidines with the helix dipole (PS-1 $\geq$ PS-2 > PS-3) as well as additional H-bonding and stacking interactions, different for PS-1 and PS-2, determine the details of helix termination and stability of these peptides. Helix stability is most pronounced for PS-2 where the helical structure extends to the carboxyamide. This is in agreement with previous studies on helix stability where electrostatic interactions provide an important factor, but where multiple additional interactions have been shown to provide non-negligible energetic contributions to the stability of helical secondary structures [4,61].

Amidation of the C-terminus has been shown to contribute to antimicrobial activity of cationic linear peptides [2,36] probably by neutralizing the otherwise acidic C-terminus. The consequences of removing the negative charge from the C-terminus are 2-fold and both may promote antimicrobial activity. First, for the same reasons as discussed above, a negative charge would result in a decrease of α-helicity due to its repulsive interactions with the negative end of the helix dipole. Second, antimicrobial activity is augmented due to the overall positive charge of the peptide which promotes interactions with the negative surface charge of bacteria [47,23,8,45]. This effect is enhanced by neutralizing the acidity of the C-terminus by amidation.

A fine balance of electrostatic [48,66] and hydrophobic interactions [71,45] is needed for membrane association and

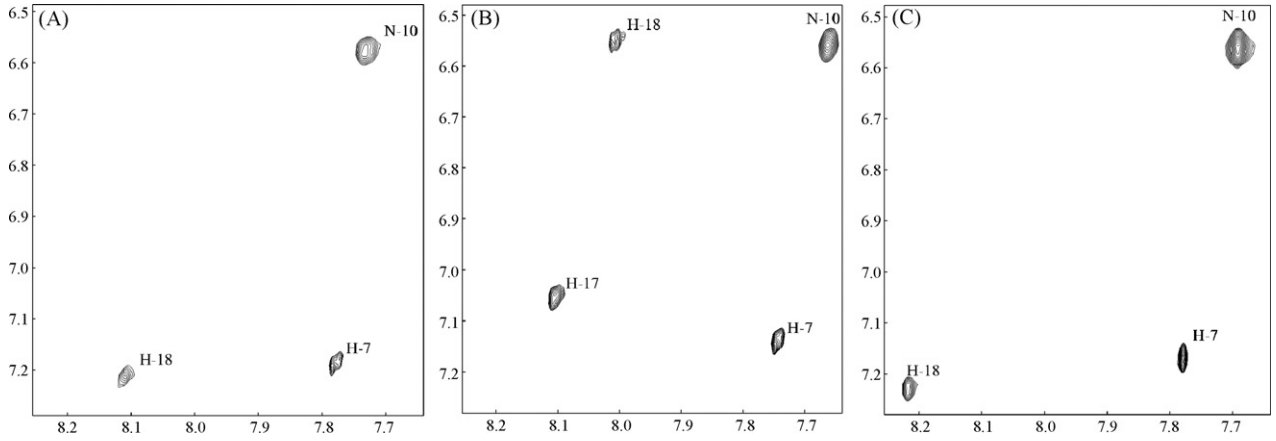

Fig. 6 – Expansions of the TOCSY spectra of PS-1 (A), PS-2 (B), and PS-3 (C) showing the ^{1}H chemical shift region of the histidine side chain correlations between H2 and H4.

Table 4 – Summary of structural statistics of PS-1, PS-2, and PS3 at 4.0 mM in TFE-d_2:H_2O (60%:40%) at 20 °C, pH 7.0 phosphate buffer

Peptide	PS-1	PS-2	PS-3
Total number of distance restrains	197	193	179
Number of intraresidue restrains	116	115	116
Number of sequential restrains (i,i + 1)	47	46	41
Number of medium range restrains $(i,i+j)_{j=2,3,4}$	34	32	22
RMSD (Å) – all residues[a]			
Backbone	1.02	1.38	2.12
Backbone and heavy atoms	1.84	2.31	3.15
RMSD (Å) – helical segment[a,b]			
Backbone	0.63	0.75	0.63
Backbone and heavy atoms	1.22	1.32	1.07
Ramachandran plot analysis[c]			
Residues in most favored regions	80.0	77.5	85.0
Residues in additional allowed regions	15.6	16.2	13.8
Residues in generously allowed regions	4.4	5.0	1.2
Residues in disallowed regions	0.0	1.2	0.0

[a] RMSD values from MOLMOL.
[b] From I-5 to N-19 for PS-1, from I-5 to F-19 for PS-2, and from I-5 to L-15 for PS-3.
[c] Data from PROCHECK_NMR.

insertion, and for the phylloseptin peptides helix formation assures the formation of amphipathic structures with a high hydrophobic moment thereby promoting membrane interactions. Furthermore, it has been shown that the coil–helix transition contributes about −0.5 kcal/mol per residue to the membrane binding energy of amphipathic peptides [70], which should promote the membrane association of PS-1 and PS-2 over PS-3. After intercalation with their helix axis parallel to the surface the peptides can develop membrane-disruptive and membrane-lytic activities or partition into the cytoplasm, thereby developing their antimicrobial activities [46,7,59,32,76].

Despite some relevant differences in secondary structures among the phylloseptins investigated, no large systematic difference in their biological activities was observed. Their activities rather vary differentially when their activities against a variety of species are compared with each other (Tables 2 and 3). This is not surprising as the fold of these structures in membrane environments is just one relevant factor for biological activity and other considerations such as aggregation in solution and in the membrane, passage through the outer bacterial layers, susceptibility to degradation by proteases, membrane binding constants as well as the detailed bilayer interactions and penetration depth are also of importance [46,7,76]. This is advantageous to the animal as the storage and secretion of cocktails of antimicrobials in the skin [27,41], makes available a larger choice and, therefore, a defense mechanism that works against many different microorganisms. At the same time releasing mixtures of antimicrobial compounds allows for the synergistic action of combinations of peptides [68,30]. Therefore, it is difficult to compare the antimicrobial activities of these peptides to the corresponding structures in membrane-mimetic environments. Nevertheless, it seems that in average PS-1 and PS-2 have slightly increased potential when compared with PS-3 (Tables 2 and 3) which correlates with the higher degree of helicity of the former peptides.

5. Conclusions

Phylloseptins exhibit antimicrobial activities against a wide range of pathogenic bacteria and fungi. The differences in sequence of Phylloseptin-1, -2, and -3 are reflected in subtle variations of the secondary structure at the C-terminus when investigated in membrane-mimetic environments using CD- and two-dimensional solution state NMR spectroscopies. Whereas the structural differences correlate with electrostatic, H-bonding and other capping interactions, amidation of the C-terminus ensures the removal of a negative charge and thereby further stabilizes the negative end of the helix dipole. The resulting amphipathic helical arrangement of these peptides thus allows them to intercalate into the bilayer interface and to develop antimicrobial activities by membrane permeabilization.

Acknowledgments

JMR thanks Conselho Nacional de Desenvolvimento Científico e Tecnológico (CNPq – Brazil) for his PhD grant and CMM thanks Coordenação de Aperfeiçoamento de Pessoal de Nível Superior (CAPES – Brazil) for her postdoctoral grant. We also thank FAPEMIG (EDT 24000) and *Vaincre la Mucoviscidose* for financial support. We acknowledge the support by the Brazilian–French program CAPES-COFECUB (487/05) who promoted this collaboration by financing several transatlantic visits.

REFERENCES

[1] Aisenbrey C, Kinder R, Goormaghtigh E, Ruysschaert JM, Bechinger B. Interactions involved in the realignment of membrane-associated helices: an investigation using oriented solid-state NMR and ATR-FTIR spectroscopies topologies. J Biol Chem 2006;281:7708–16.
[2] Ali MF, Soto A, Knoop FC, Conlon JM. Antimicrobial peptides isolated from skin secretions of the diploid frog, *Xenopus tropicalis* (Pipidae). Biochim Biophys Acta 2001;1550:81–9.
[3] Apponyi MA, Pukala TL, Brinkworth CS, Maselli VM, Bowie JH, Tyler MJ, et al. Host-defence peptides of Australian anurans: structure, mechanism of action and evolutionary significance. Peptides 2004;25:1035–54.
[4] Armstrong KM, Baldwin RL. Charged histidine affects alpha-helix stability at all positions in the helix by interacting with the backbone charges. Proc Natl Acad Sci U S A 1993;90:11337–40.
[5] Aurora R, Rose GD. Helix capping. Protein Sci 1998;7:21–38.
[6] Bax A, Davis DG. MLEV-17-based two-dimensional homonuclear magnetization transfer spectroscoy. J Magn Res 1985;65:355–60.

[7] Bechinger B. The structure, dynamics and orientation of antimicrobial peptides in membranes by solid-state NMR spectroscopy. Biochim Biophys Acta 1999;1462:157–83.
[8] Bechinger B. Membrane-lytic peptides. Crit Rev Plant Sci 2004;23:271–92.
[9] Bechinger B, Lohner K. Detergent-like action of linear cationic membrane-active antibiotic peptides. Biochim Biophys Acta 2006;1758:1529–39.
[10] Bechinger B, Zasloff M, Opella SJ. Structure and orientation of the antibiotic peptide magainin in membranes by solid-state NMR spectroscopy. Protein Sci 1993;2:2077–84.
[11] Bhattacharyya R, Samanta U, Chakrabarti P. Aromatic–aromatic interactions in and around alpha-helices. Protein Eng 2002;15:91–100.
[12] Boman HG. Antibacterial peptides: basic facts and emerging concepts. J Intern Med 2003;254:197–215.
[13] Brand GD, Leite JR, de Sa Mandel SM, Mesquita DA, Silva LP, Prates MV, et al. Novel dermaseptins from *Phyllomedusa hypochondrialis* (Amphibia). Biochem Biophys Res Commun 2006;347:739–46.
[14] Brogden KA. Antimicrobial peptides: pore formers or metabolic inhibitors in bacteria? Nat Rev Microbiol 2005;3:238–50.
[15] Bulet P, Cociancich S, Dimarcq JL, Lambert J, Reichhart JM, Hoffmann D, et al. Insect immunity. Isolation from a coleopteran insect of a novel inducible antibacterial peptide and of new members of the insect defensin family. J Biol Chem 1991;266:24520–5.
[16] Butterfield SM, Patel PR, Waters ML. Contribution of aromatic interactions to alpha-helix stability. J Am Chem Soc 2002;124:9751–5.
[17] Caffrey MS, Cusanovich MA. Lysines in the amino-terminal alpha-helix are important to the stability of *Rhodobacter capsulatus* cytochrome c2. Biochemistry 1991;30:9238–41.
[18] Carver JA, Collins JG. NMR identification of a partial helical conformation for bombesin in solution. Eur J Biochem 1990;187:645–50.
[19] Cavanagh J, Fairbrother WJ, Palmer III AG, Skelton NJ, Protein NMR Spectroscopy, Principles and Practice; 1996; Academic Press, San Diego.
[20] Chan WC, White SH. Fmoc solid-phase peptide synthesis: a practical approach; 2000; Oxford University Press, New York.
[21] Chelli R, Gervasio FL, Procacci P, Schettino V. Stacking and T-shape competition in aromatic–aromatic amino acid interactions. J Am Chem Soc 2002;124:6133–43.
[22] Chen YH, Yang JT, Chau KH. Determination of the helix and β form of proteins in aqueous solution by circular dichroism. Biochemistry 1974;13:3350–9.
[23] Dathe M, Schümann M, Wieprecht T, Winkler A, Beyermann M, Krause E, et al. Peptide helicity and membrane surface charge modulate the balance of electrostatic and hydrophobic interactions with lipid bilayers and biological membranes. Biochemistry 1996;35:12612–2.
[24] Delaglio F, Grzesiek S, Vuister GW, Zhu G, Pfeifer J, Bax A. NMRPipe: a multidimensional spectral processing system based on UNIX pipes. J Biomol NMR 1995;6:277–93.
[25] Derome AE, Williamson MP. Rapid-pulsing artifacts in double-quantum filtered COSY. J Magn Reson 1990;88:177–85.
[26] Duclohier H, Molle G, Spach G. Antimicrobial peptide magainin I from *Xenopus* skin forms anion-permeable channels in planar lipid bilayers. Biophys J 1989;56:1017–21.
[27] Giovannini MG, Poulter L, Gibson BW, Williams DH. Biosynthesis and degradation of peptides derived from *Xenopus laevis* prohormones. Biochem J 1987;243:113–20.
[28] Hancock RE, Sahl HG. Antimicrobial and host-defense peptides as new anti-infective therapeutic strategies. Nat Biotechnol 2006;24:1551–7.
[29] Hancock RE, Scott MG. The role of antimicrobial peptides in animal defenses. Proc Natl Acad Sci U S A 2000;97:8856–61.
[30] Hara T, Mitani Y, Tanaka K, Uematsu N, Takakura A, Tachi T, et al. Heterodimer formation between the antimicrobial peptides magainin 2 and PGLa in lipid bilayers: a cross-linking study. Biochemistry 2001;40:12395–9.
[31] Holak TA, Engstrom A, Kraulis PJ, Lindeberg G, Bennich H, Jones TA, et al. The solution conformation of the antibacterial peptide cecropin A: a nuclear magnetic resonance and dynamical simulated annealing study. Biochemistry 1988;27:7620–9.
[32] Huang HW. Action of antimicrobial peptides: two-state model. Biochemistry 2000;39:8347–52.
[33] Hwang PM, Vogel HJ. Structure–function relationships of antimicrobial peptides. Biochem Cell Biol 1998;76: 235–46.
[34] Hyberts SG, Goldberg MS, Havel TF, Wagner G. The solution structure of eglin C based on measurements of many NOEs and coupling constants and its comparison with X-ray structures. Protein Sci 1992;1:736–51.
[35] Johnson BA, Blevins RA. NMRVIEW: a computer program for the visualization and analysis of NMR data. J Biomol NMR 1994;4:603–14.
[36] Katayama H, Ohira T, Aida K, Nagasawa H. Significance of a carboxyl-terminal amide moiety in the folding and biological activity of crustacean hyperglycemic hormone. Peptides 2002;23:1537–46.
[37] Koradi R, Billeter M, Wüthrich K. MOLMOL: a program for display and analysis of macromolecular structures. J Mol Graph 1996;14:51–5.
[38] Kuchinka E, Seelig J. Interaction of melittin with phosphatidylcholine membranes. Binding isotherm and lipid head-group conformation. Biochemistry 1989;28: 4216–21.
[39] Kumar A, Ernst RR, Wüthrich K. A two-dimensional nuclear Overhauser enhancement (2D NOE) experiment for the elucidation of complete proton–proton cross-relaxation networks in biological macromolecules. Biochem Biophys Res Commun 1980;95:1–6.
[40] Laskowski RA, Rullmannn JA, MacArthur MW, Kaptein R, Thornton JM. AQUA and PROCHECK-NMR: programs for checking the quality of protein structures solved by NMR. J Biomol NMR 1996;8:477–86.
[41] Leite JR, Silva LP, Rodrigues MI, Prates MV, Brand GD, Lacava BM, et al. Phylloseptins: a novel class of anti-bacterial and anti-protozoan peptides from the *Phyllomedusa* genus. Peptides 2005;26:565–73.
[42] Marion D, Zasloff M, Bax A. A two-dimensional NMR study of the antimicrobial peptide magainin 2. FEBS Lett 1988;227:21–6.
[43] Markley JL. Observation of histidine residues in proteins nuclear magnetic resonance spectroscopy. Acc Chem Res 1975;8:70–80.
[44] Mason AJ, Gasnier C, Kichler A, Prevost G, Aunis D, Metz-Boutigue MH, et al. Enhanced membrane disruption and antibiotic action against pathogenic bacteria by designed histidine-rich peptides at acidic pH. Antimicrob Agents Chemother 2006;50:3305–11.
[45] Mason AJ, Martinez A, Glaubitz C, Danos O, Kichler A, Bechinger B. The antibiotic and DNA transfecting peptide LAH4 selectively associates with, and disorders, anionic lipids in mixed membranes. FASEB J 2005;20:320–2.
[46] Matsuzaki K. Magainins as paradigm for the mode of action of pore forming polypeptides. Biochim Biophys Acta 1998;1376:391–400.
[47] Matsuzaki K, Harada M, Handa T, Funakoshi S, Fujii N, Yajima H, et al. Magainin 1-induced leakage of entrapped calcein out of negatively-charged lipid vesicles. Biochim Biophys Acta 1989;981:130–4.

[48] Matsuzaki K, Nakamura A, Murase O, Sugishita K, Fujii N, Miyajima K. Modulation of magainin 2-lipid bilayer interactions by peptide charge. Biochemistry 1997;36: 2104–11.
[49] McGaughey GB, Gagne M, Rappe AK. pi-Stacking interactions. Alive and well in proteins. J Biol Chem 1998;273:15458–63.
[50] Novak R, Henriques B, Charpentier E, Normark S, Tuomanen E. Emergence of vancomycin tolerance in *Streptococcus pneumoniae*. Nature 1999;399:590–3.
[51] Park CB, Kim MS, Kim SC. A novel antimicrobial peptide from *Bufo bufo* gargarizans. Biochem Biophys Res Commun 1996;218:408–13.
[52] Piantini U, Sorensen OW, Bodenhausen G, Ernst RR. Multiple quantum filters for elucidating NMR coupling networks. J Am Chem Soc 1982;104:6800–1.
[53] Piotto M, Saudek V, Sklenar V. Gradient-tailored excitation for single-quantum NMR spectroscopy of aqueous solutions. J Biomol NMR 1992;2:661–5.
[54] Prieto J, Serrano L. C-capping and helix stability: the Pro C-capping motif. J Mol Biol 1997;274:276–88.
[55] Prongidi-Fix L, Sugewara M, Bertani P, Raya J, Leborgne C, Kichler A, et al. Self-promoted uptake of peptide/DNA transfection complexes. Biochemistry 2007;46:11253–62.
[56] Pukala TL, Bowie JH, Maselli VM, Musgrave IF, Tyler MJ. Host-defence peptides from the glandular secretions of amphibians: structure and activity. Nat Prod Rep 2006;23:368–93.
[57] Sadler PJ, Tucker A. pH-induced structural transitions of bovine serum albumin. Histidine pK_a values and unfolding of the N-terminus during the N to F transition. Eur J Biochem 1993;212:811–7.
[58] Schwieters CD, Kuszewski JJ, Tjandra N, Clore GM. The Xplor-NIH NMR molecular structure determination package 1996. J Magn Res 2003;160:65–73.
[59] Shai Y. Mechanism of the binding, insertion, and destabilization of phospholipid bilayer membranes by alpha-helical antimicrobial and cell non-selective lytic peptides. Biochim Biophys Acta 1999;1462:55–70.
[60] Shai Y. Mode of action of membrane active antimicrobial peptides. Biopolymers 2002;66:236–48.
[61] Shi Z, Olson CA, Bell Jr AJ, Kallenbach NR. Stabilization of alpha-helix structure by polar side-chain interactions: complex salt bridges, cation-pi interactions, and C-H em leader O H-bonds. Biopolymers 2001;60:366–80.
[62] Simmaco M, Mignogna G, Barra D. Antimicrobial peptides from amphibian skin: what do they tell us? Biopolymers 1998;47:435–50.
[63] Sreerama N, Woody RW. Estimation of protein secondary structure from circular dichroism spectra: comparison of CONTIN, SELCON, and CDSSTR methods with an expanded reference set. Anal Biochem 2000;252–60.
[64] Steiner H, Hultmark D, Engstrom A, Bennich H, Boman HG. Sequence and specificity of two antibacterial proteins involved in insect immunity. Nature 1981;292:246–8.
[65] Sun S, Bernstein ER. Aromatic van der Waals clusters: structure and nonrigidity. J Phys Chem 1996;100: 13348–66.
[66] Vogt TCB, Bechinger B. The interactions of histidine-containing amphipathic helical peptide antibiotics with lipid bilayers: the effects of charges and pH. J Biol Chem 1999;274:29115–21.
[67] Wayne P. Performance standards for antimicrobial susceptibility testing, NCCLS-approved standard M100-S9; 1999.
[68] Westerhoff HV, Zasloff M, Rosner JL, Hendler RW, de Waal A, Vaz Gomes A, et al. Functional synergism of the magainins PGLa and magainin-2 in *Escherichia coli*, tumor cells and liposomes. Eur J Biochem 1995;228:257–64.
[69] White SH, Wimley WC. Membrane protein folding and stability: physical principles. Annu Rev Biophys Biomol Struct 1999;28:319–65.
[70] Wieprecht T, Apostolov O, Beyermann M, Seelig J. Thermodynamics of the alpha-helix-coil transition of amphipathic peptides in a membrane environment: implications for the peptide-membrane binding equilibrium. J Mol Biol 1999;294:785–94.
[71] Wieprecht T, Dathe M, Krause E, Beyermann M, Maloy WL, MacDonald DL, et al. Modulation of membrane activity of amphipathic, antibacterial peptides by slight modifications of the hydrophobic moment. FEBS Lett 1997;417:135–40.
[72] Wilker W, Leibfritz D, Kerssebaum R, Bernel W. Gradient selection in inverse heteronuclear spectroscopy. Magn Reson Chem 1993;31:287–92.
[73] Wishart DS, Sykes BD, Richards FM. The chemical shift index: a fast and simple method for the assignment of protein secondary structure through NMR spectroscopy. Biochemistry 1992;31:1647–51.
[74] Wüthrich K. NMR of Proteins and Nucleic Acids; 1986.
[75] Zasloff M. Magainins, a class of antimicrobial peptides from *Xenopus* skin: isolation, characterization of two active forms, and partial cDNA sequence of a precursor. Proc Natl Acad Sci U S A 1987;84:5449–53.
[76] Zasloff M. Antimicrobial peptides of multicellular organisms. Nature 2002;415:389–95.